J Fluoresc (2012) 22:349–355
DOI 10.1007/s10895-011-0965-5

ORIGINAL PAPER

Label-Free Spatial Analysis of Free and Enzyme-Bound NAD(P)H in the Presence of High Concentrations of Melanin

Sebastian Herbrich · Matthias Gehder · Rainer Krull · Karl-Heinz Gericke

Received: 18 May 2011 / Accepted: 30 August 2011 / Published online: 6 September 2011

Abstract The analysis of autofluorescence, often regarded as undesired noise during the imaging of biological samples, allows label free, unbiased detection of NAD(P)H and melanin in native samples. Because both the emission and absorption spectra of these fluorophores overlap and they can hence not be differentiated using emission filters or with different excitation wavelengths, fluorescence lifetime imaging microscopy (FLIM) is used to differentiate between them. In the present paper the application of two-photon excitation microscopy is presented to investigate the autofluorescence of fungal spores. The model organism which was examined is A*spergillus ochraceus*. Furthermore a strategy is developed which allows to quantitatively analyze the fluorescence lifetimes of melanin, free NAD(P)H and protein-bound NAD(P)H using forward convolution of a multiexponential decay function with the instrument response function (IRF) and subsequent fitting to the experimental fluorescence data. As a consequence proteins, which are able to bind NAD(P)H, are located with sub-cellular resolution. Furthermore a spatial differentiation of the fluorophores NAD(P)H and melanin inside the spores, is revealed.

S. Herbrich · K.-H. Gericke (✉)
Institute of Physical and Theoretical Chemistry,
Technische Universität Braunschweig,
Hans-Sommerstraße 10,
38106 Braunschweig, Germany
e-mail: k.gericke@tu-bs.de

M. Gehder · R. Krull
Institute of Biochemical Engineering,
Technische Universität Braunschweig,
Gaußstraße 17,
38106 Braunschweig, Germany

Keywords NAD(P)H · Melanin · Spore · Fluorescence lifetime imaging · Forward convolution

Introduction

Intrinsic fluorescence has become an important assay in various biologically relevant studies as it reveals the characteristics of a sample in its natural environment [1]. The most relevant biological intrinsic fluorophores for cells are NAD(P)H, retinol, indoleamines, collagen, melanin and chlorophyll [2–6]. It is also possible to obtain the intrinsic fluorescence of proteins and use it for label-free experiments as we have shown before [7]. In general, fluorophores can be distinguished by their absorption and emission spectra. Sometimes, however, the emission spectra overlap and a spectral discrimination is not possible. For instance NAD(P)H absorbs radiation around 350 nm which overlaps with the absorption spectra of melanin [8] and the emission of both molecules is also in the same spectral range. However, their fluorescence lifetimes are different allowing one to distinguish between them. One can even differentiate between free and enzyme-bound NAD(P)H as was shown by Lakowicz et al. [9]. Moreover it is possible to perform morphological studies of biological samples by using the distribution of the fluorescence lifetime if the intrinsic fluorophores are located in specific areas of the sample [10, 11].

A good way to determine the fluorescence lifetime is the use of two-photon excitation (TPE) experiments combined with either time correlated single photon counting (TCSPC) or time gated techniques [12–15]. TPE has several advantages over simple one-photon excitation and it is one of the most used techniques currently used for bio-imaging [16]. The most important advantage of TPE over

one-photon excitation is that the excitation itself is limited to the focal volume. Therefore, the photodamage is strongly reduced outside of the focal volume and a better contrast can be achieved [17].

In the present study it is demonstrated that the combination of TPE and a forward convolution of a multiexponential decay function is able to discriminate between free and protein-bound NAD(P)H as well as melanin and that it is even possible to determine the relative concentration of free and enzyme-bound NAD(P)H. As a model organism a member of the A*spergillus* family as their dark color is indicative of relative high concentrations of melanin has been chosen. Nevertheless, it will be shown that free and enzyme-bound NAD(P)H can be detected with sub-cellular resolution.

In general short fluorescence lifetimes are difficult to evaluate as they might interfere with the instrumental response function (IRF) of the experimental setup. This is the case for the fluorescence lifetime of melanin, which is reported to be about 30 to 40 ps [18]. Therefore it is important to measure the IRF and integrate it into the evaluation of the data as has been done for the present analysis.

Material and Methods

For the generation of assessable spores, malt extract agar plates were inoculated with *Aspergillus ochraceus* cultures (strain DSM 63304) for 8 d in the dark at 24 °C. Spores were harvested through the addition of 25 mL sterile saline solution and sheering with glass beads. The obtained suspension was strained through a miracloth filter (25 μm mesh width). Microscope slides and cover slips were silanized for increased hydrophobicity with chloroform containing 5% dimethyldichlorosilane, dried overnight and heated at 180 °C for 2 h.

The experimental setup is shown in Fig. 1. The fundamental of a Ti:Sa laser (Mira 900 D, Coherent, Santa Clara, CA) was focused through a water objective (C-Apochromat 40x, NA 1.2, ZEISS, Jena, Germany) on the sample. Scanning of the sample was achieved through a piezo driven table (Physik Instrumente GmbH, Karlsruhe, Germany). The emission light of the sample was filtered through a short-pass filter (BG 39, Schott, Mainz, Germany) and a short-pass emission filter (FF01-460/80, Semrock). It was detected by a single photon avalanche diode (PDM series, MPD, Bolzano, Italy) which was connected to a TCSPC device (Picoharp 300, PicoQuant GmbH, Berlin, Germany). The data were recorded via SymPhoTime (V 5.2.3.2, PicoQuant GmbH, Berlin, Germany) and exported as a pre-histogram image. The analysis of the fluorescence image was performed with self written code utilizing MATLAB 2010b, which is published in the supplement.

Results and Discussion

Analyzing the Fluorescence Data

The fluorescence signal I(t) which is observed in the experiment is obtained from a convolution of the sample fluorescence F(t) with the instrumental response function IRF(t') resulting in Eq. 1 with *t*' as an integration parameter.

$$I(t) = \int_{-\infty}^{\infty} IRF(t') \cdot F(t - t')dt' \tag{1}$$

A simplification can be done to the upper interval due to the fact that there is no fluorescence signal before the excitation pulse. If the laser pulse defines the time t, it has been obtained:

$$I(t) = \int_{-\infty}^{t} IRF(t') \cdot F(t - t')dt' \tag{2}$$

The IRF needs to be determined experimentally and there are several ways to obtain the IRF of an experimental setup [19]. We have chosen to use the white light generation in paraffin in order to generate a fast event F(t) the duration of which is short compared to the IRF. White light generation by focusing 800 nm light into a medium is a non-linear effect which is mainly used for pump-probe experiments or for photonic crystal fibers to generate short femtosecond pulses on a large spectral range (350–600 nm) [20]. Since the IRF of the APD detector is wavelength dependent the generated white light was filtered through the same fluorescence filter used in the experiment to obtain the appropriate IRF. The IRF obtained for our setup is shown in Fig. 2. It complies with the IRF of the official datasheet of the APD [21].

As a result of intermolecular binding the intrinsic fluorophores can occur in several different forms, each one with a characteristic fluorescence decaytime τ_j. Therefore, the fluorescence signal F(t) can be expressed as the sum of exponential functions, each representing the fluorescence decay of a single fluorophore. As a result it is possible to extract a variety of fluorescence lifetimes τ_j from the measurement as indicated in Eq. 3.

$$I_{ik}(t) = I_0 + \int_{-\infty}^{t} IRF(t') \cdot \sum_{j=1}^{n} a_j(i,k) \cdot e^{\frac{-(t-t')}{\tau_j}} dt' \tag{3}$$

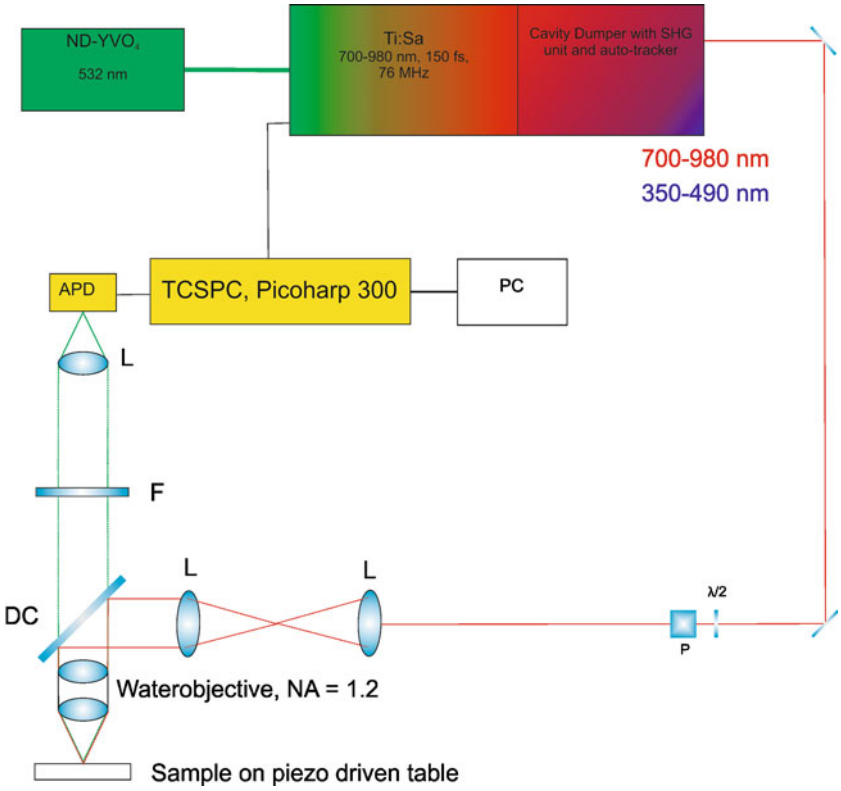

Fig. 1 Experimental setup; λ/2: lambda-half-waveplate; P: polarizer; L: lens; DC: dichroic-mirror; F: emission filter; APD: avalanche-photo-diode

I_0 is the background signal and the $a_j(i, k)$ are the intensity contributions of every single exponential fluorescence lifetime τ_j to the overall fluorescence signal $I_{ik}(t)$ for each pixel (i,k) of the fluorescence image.

In a first step, a global tri-exponential fit (n=3; Eq. 3) of $I(t) = \sum_{i,k} I_{ik}(t)$ was performed in order to determine the three relevant lifetimes τ_1, τ_2 and τ_3. The tri-exponential form was utilized because three fluorescence lifetimes represent the molecules under consideration: τ_1, a very short one from melanin in the cell wall, τ_2, a longer one for the free form of NAD(P)H and τ_3, a much longer one for the protein-bound of NAD(P)H.

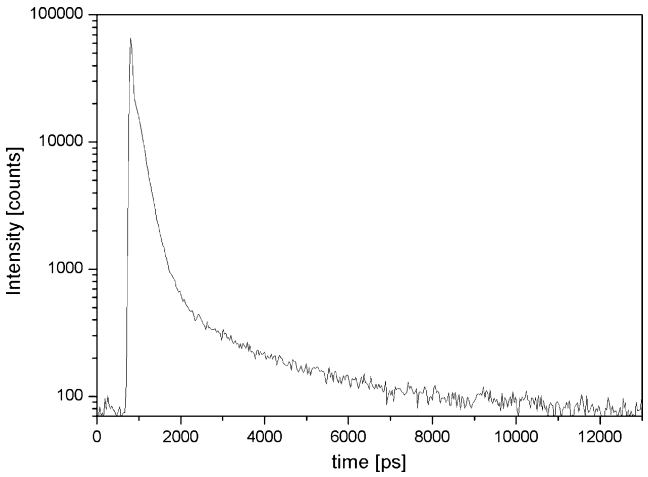

Fig. 2 IRF (FWHM 72 ps) generated by focusing 800 nm femtosecond pulses into paraffin in order to generate white light which then was filtered through a short-pass Schott BG 39 filter and a short-pass emission filter (FF01-460/80, Semrock)

After the determination of the three lifetimes τ_1, τ_2 and τ_3 a local fit for each pixel was performed in a second step where, again, the IRF was considered according to Eq. 3. Here the fluorescence lifetimes τ_j of the global fit where used as fixed parameters. Therefore, one obtains the contribution of each fluorescence lifetime τ_j to the total fluorescence decay, i.e. the $a_j(ik)$ for each pixel (Eq. 3). The received data were depicted as a normalized fluorescence lifetime image in which three different colors were used for the three lifetimes to reveal the localization of melanin, free and protein-bound NAD(P)H.

Fit Results

There are several challenges examining biological samples as their intrinsic fluorophores can be found in various isoforms, each characterized by a different fluorescence lifetime. Particularly melanin shows a complex fluorescence decay. Forest et al. [22] report of a maximum of four different fluorescence lifetimes for melanin. In general, melanin got one dominant short fluorescence

lifetime about 30 to 40 ps as Ehlers et al. [18] have reported while investigating hair samples. Therefore, it is expected that the shortest fluorescence lifetime τ_1 which has been determined is from melanin. It is localized in the cell wall [5]. Free and protein-bound NAD(P)H, however, were identified through comparison with previously published data where the fluorescence lifetime of the free coenzyme was reported to be around 500 ps and that of the bound cofactor around 3 ns, slightly varying depending on cell conditions [9–11, 23].

The global fit and residuals are shown in Fig. 3 and the results are represented in Table 1. The shortest observed fluorescence lifetime τ_1 of 32 ps originates from melanin which is in good agreement with previously published data [18]. The quantitative determination of this value is difficult as the time resolution of the applied APDs is 72 ps at the wavelength range of the employed short-pass filter (460± 80 nm). Although the τ_1 value is actually below the time resolution of the experimental set-up an accuracy of about 10 ps can be obtained for this short lifetime due to the fit of the forward convolution according to Eq. 3. In general, this accuracy depends significantly on the time resolution of the experimental setup, the accuracy of the IRF and the signal to-noise ratio. We analyzed more than hundred different probes and found that the variation for the shortest lifetime is within 10 ps.

The two longer fluorescence lifetimes 488 ps (τ_2) and 3.5 ns (τ_3) are caused by free and protein-bound NAD(P)H, respectively and are in good agreement with previously published values [9, 23]. However, it should be mentioned that the lifetime τ_3 depends on the protein(s) to which this cofactor is bound. Although the identity of these NAD(P)H binding proteins remains unknown, it is possible to localize regions of increased concentrations on a sub-cellular level.

Table 1 Analyzed fluorescence lifetimes and their contributions to the total fluorescence

Parameter index j	Fluorescence lifetime τ_j/ps	Intensity contribution A_j/ 10^4 counts
1	32±10	175±25
2	490±140	2.00±0.60
3	3530±190	1.13±0.10

Figure 4 shows a typical total fluorescence decay I(t) of a spore of *A. ochraceus* and how the three single fluorescence lifetimes contribute to it. The shortest lifetime τ_1 is only detectable immediately after the excitation pulse and comparable to the time resolution of the experimental setup. Therefore, it is necessary to pay attention to the IRF and take it into account as shown before in Eq. 1. The fluorescence lifetimes τ_2 and τ_3 are not highly dependent on the IRF as they are much longer than the FWHM of the IRF. Nevertheless, for an accurate quantitative value it is important to consider the IRF according to Eq. 3. Figure 4 suggests that there might be an additional decay curve in the time range above 4 ns, however, this part merely represents the background I_0 of the fluorescence signal which was taken into account during the fitting procedure (Eq. 3).

An important value is A_j, which is the sum of $a_j(i, k)$ over the whole fluorescence image, it can be used to obtain the relative contributions of melanin (τ_1), free NAD(P)H

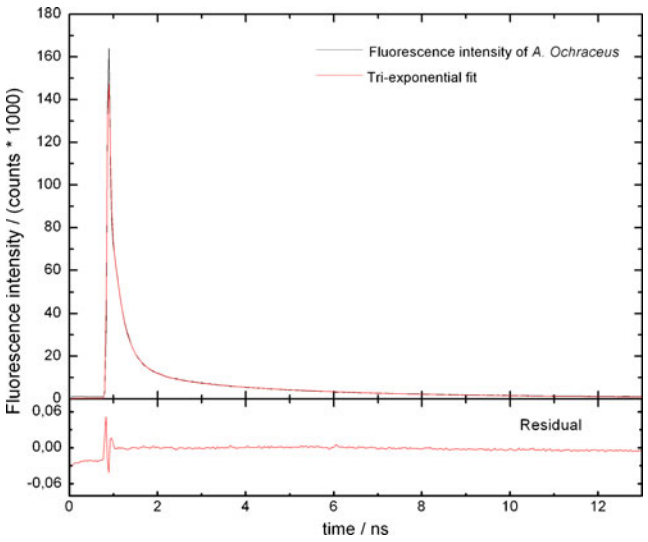

Fig. 3 Fluorescence decay of *Aspergillus ochraceus* with a tri-exponential fit and its residual. The deviation of the residual at longer times (>4,000 ps) from the fit are due to a constant background signal I_0 (Eq. 3)

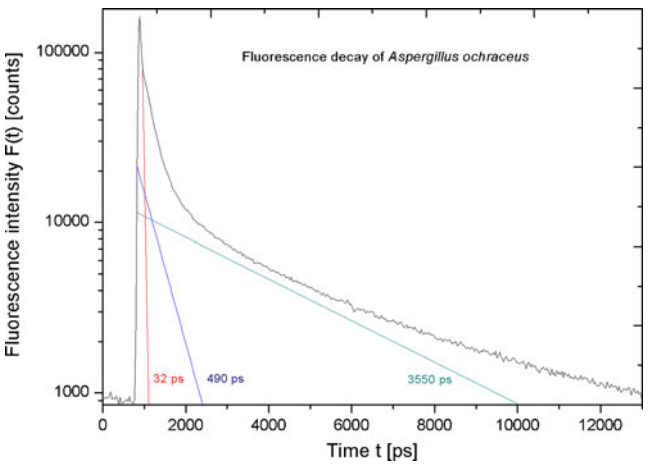

Fig. 4 Total fluorescence decay of *Aspergillus ochraceus* and its 3 different fluorescence lifetimes. The deviation of the fluorescence intensity at longer times (>4,000 ps) from the 3550 ps-line are due to a constant background signal I_0 (Eq. 3)

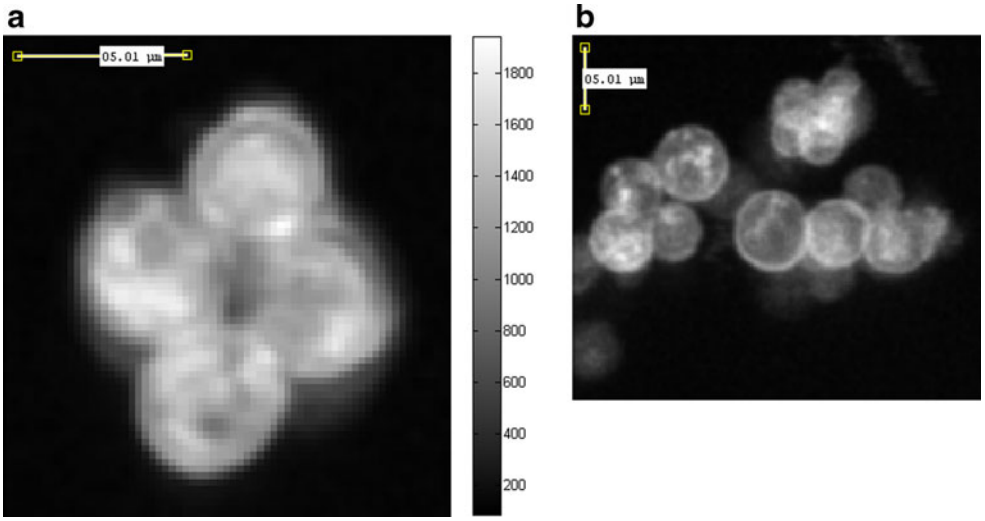

Fig. 5 Intensity images of the autofluorescence of *Aspergillus ochraceus*

(τ_2) and enzyme-bound NAD(P)H (τ_3) to the total fluorescence signal.

$$A_j = \sum_{i,k} a_j(i,k) \tag{4}$$

The fit results for A_j listed in Table 1 show that the contribution A_1 of the shortest fluorescence lifetime τ_1 is two magnitudes higher than that of A_2 and A_3: $A_1 / \sum_{j=1}^{3} A_j = 0.99$

However, this fluorescence occurs mainly in the cell wall. Arcangeli et al. [24] reported a similar behavior in the Antarctic fungus *Arthrobotrys ferox*. They reported that the cell wall-membrane fluorophores were responsible for the higher intensity of the wall in contrast to the inner region but they were not able to specify their findings nor have they determined any fluorescence lifetimes. Further examinations of the cell wall have shown that the short lifetime τ_1 dominates this area and no NAD(P)H could be found there.

Figure 5 shows the fluorescence intensity of different samples of *A. ochraceus*. The left part of Fig. 5 shows the fluorescence of 4 spores while the right part shows another area of the sample using lower magnification. One can even see the lower layer of spores underneath the brighter spores. While a spatial distinction between the single spores is possible in the left image of Fig. 5, it becomes more difficult in the top right corner of the right image of Fig. 5. One can obtain a much better spatial resolution if instead of an intensity mapping a fluorescence lifetime

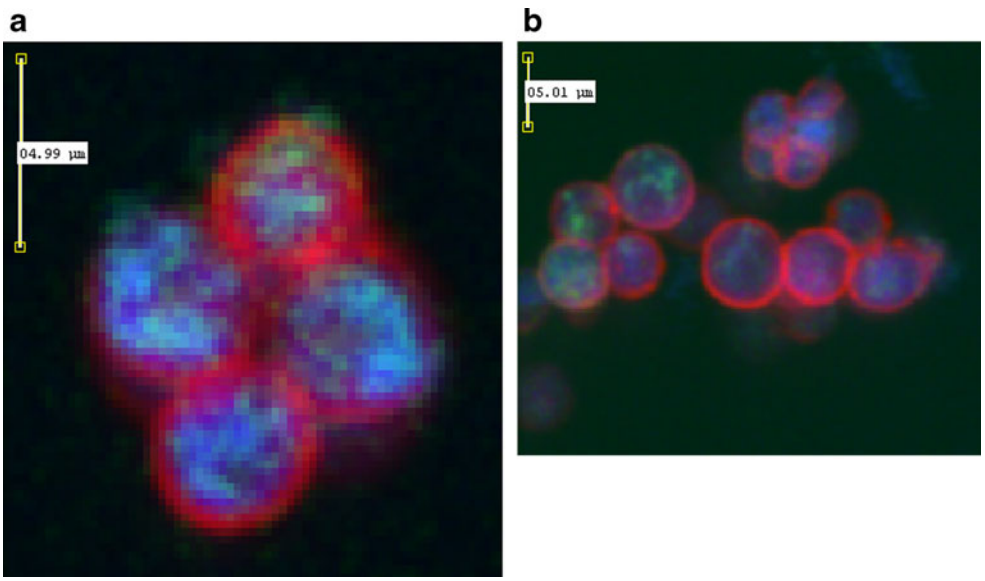

Fig. 6 Fluorescence lifetime images of *Aspergillus ochraceus.* An RGB color code is applied where red represents the fluorescence lifetime of melanin (τ_1), green represents the fluorescence lifetime of free NAD(P)H (τ_2) and blue represents the fluorescence lifetime of protein-bound NAD(P)H (τ_3)

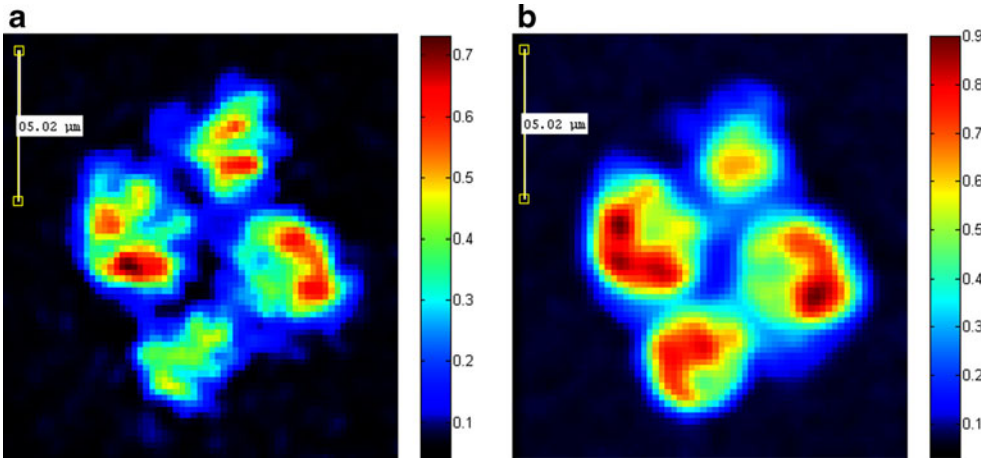

Fig. 7 left: Distribution of free NAD(P)H; right: Distribution of enzyme-bound NAD(P)H

image is used as is shown in Fig. 6. An RGB color code is applied where red represents the shortest fluorescence lifetime τ_1, melanin, green represents the fluorescence lifetime τ_2, free NAD(P)H, and blue represents the longest fluorescence lifetime τ_3, protein-bound NAD(P)H. The distribution of the A_j (j=1,2,3) were individually normalized over all pixels of the image for a better visualization of the melanin, free and enzyme-bound NAD(P)H distribution within the spore. Melanin (red) appears mainly in the cell wall while free NAD(P)H (green) and enzyme-bound NAD(P)H (blue) overlap frequently. It is still problematic to recognize the distribution of NAD(P)H from this image. Therefore, two additional images were generated from the fitted data, which show individual contributions of free (a_1(i,k)=0; a_2(ik); a_3(i,k)=0; Fig. 5 left) and enzyme-bound NAD(P)H (a_1(i,k)=0; a_2(i,k)=0; a_3(ik); Fig. 5 right). A new colormap is used for better visualization. Figure 7 indicates that the NAD(P)H is not equally distributed. There are small areas in which enzyme-bound NAD(P)H clearly dominates while it is hardly found in other parts of the spore. Although one cannot distinguish between the proteins that bind NAD(P)H their localization is readily possible with the here presented methods.

Summary

The present paper characterizes the intrinsic fluorescence of fungal spores using the technique of two-photon microscopy. Although, the emission and absorption spectra of NAD(P)H and melanin show a large overlap and it is not possible to differentiate between the two molecules by classical spectroscopy. It has been shown that a discrimination can be done by utilizing fluorescence lifetimes in confluence with considering the influence of the instrumental response function. A forward convolution method was applied to obtain quantitative data of the fluorescence lifetimes on the picosecond scale. Although, the contribution of the melanin fluorescence is 99% to the total fluorescence signal, our study reveals the spatial separation of melanin and NAD(P)H within spores of the filamentous fungus *Aspergillus ochraceus*.

Very little is known about the compartmentalization of spores. In most cases it is expected that they lack any compartments as they represent the most “condensed form of life”. The here presented findings, however, are indicative of a well organized inner structure of fungal spores. Especially Fig. 7 shows, that there is a clear difference between regions of spores that contain higher concentrations of protein-bound NAD(P)H and those with primarily free NAD(P)H. As the ratio of protein-bound and free NAD(P)H is an indicator for the metabolic activity and metabolic readiness, this implies that the metabolic activity of spores is carried out in distinct regions of the same. Whether or not they are (contrary to the currently expected) surrounded by intracellular membranes needs to be investigated in future studies. The fact itself that there is some sort of organization within the spore is yet remarkable and completely new. It also shows that there must be some sort of spatial organizational instance. This could be, but is not limited to, proteinogenic or lipid structures.

The localization of proteins that bind NAD(P)H is obtained with sub-cellular resolution due to the relative contribution of the fluorescence lifetimes to the total fluorescence decay. It is demonstrated that the technique presented here is applicable for the assessment of NAD(P)H and melanin in all biological samples, even those with high concentrations of melanin.

Acknowledgements Financial support by the Deutsche Forschungsgemeinschaft (SH) and the German National Merit Foundation (MG) are kindly acknowledged. The authors also thank PicoQuant GmbH for material support. Support of the IGSM Braunschweig is also gratefully acknowledged.

References

1. Lakowicz JR (2006) Principles of fluorescence spectroscopy. Vol, 3rd edn. Springer, New York
2. Baker NR (2008) Chlorophyll fluorescence: a probe of photosynthesis in vivo. Annu Rev Plant Biol 59(1):89–113
3. Imanishi Y, Lodowski KH, Koutalos Y (2007) Two-photon microscopy: shedding light on the chemistry of vision†. Biochemistry 46(34):9674–9684
4. Meredith P, Sarna T (2006) The physical and chemical properties of eumelanin. Pigment Cell Res 19(6):572–594
5. Durrell LW (1964) The composition and structure of walls of dark fungus spores. Mycopathologia 23(4):339–345
6. Bell AA, Wheeler MH (1986) Biosynthesis and functions of fungal melanins. Annu Rev Phytopathol 24(1):411–451
7. Quentmeier S, Quentmeier CC, Walla PJ, Gericke K-H (2009) Two-color two-photon excitation of intrinsic protein fluorescence: label-free observation of proteolytic digestion of bovine serum albumin. Chemphyschem 10(9–10):1607–1613
8. Tran ML, Powell BJ, Meredith P (2006) Chemical and structural disorder in eumelanins: a possible explanation for broadband absorbance. Biophys J 90(3):743–752
9. Lakowicz JR, Szmacinski H, Nowaczyk K, Johnson ML (1992) Fluorescence lifetime imaging of free and protein-bound NADH. Proc Natl Acad Sci USA 89(4):1271–1275
10. Niesner R, Narang P, Spiecker H, Andresen V, Gericke K-H, Gunzer M (2008) selective detection of NADPH oxidase in polymorphonuclear cells by means of NAD(P)H-based fluorescence lifetime imaging. J Biophys, 2008
11. Niesner R, Bülent P, Schlüsche P, Gericke K-H (2004) Non-iterative biexponential fluorescence lifetime imaging in the investigation of cellular metabolism by means of NAD(P)H autofluorescence. Chemphyschem 5(8):1141–1149
12. Elson D et al (2004) Time-domain fluorescence lifetime imaging applied to biological tissue. Photochem Photobiol Sci 3(8):795–801
13. Gerritsen HC, Asselbergs MAH, Agronskaia AV, Van Sark WGJHM (2002) Fluorescence lifetime imaging in scanning microscopes: acquisition speed, photon economy and lifetime resolution. J Microsc 206(3):218–224
14. Niesner R, Gericke K-H (2008) Fluorescence lifetime imaging in biosciences: technologies and applications. Front Phys 3(1)
15. Denicke S, Ehlers J-E, Niesner R, Quentmeier S, Gericke K-H (2007) Steady-state and time-resolved two-photon fluorescence microscopy: a versatile tool for probing cellular environment and function. Phys Scripta 76(3):C115
16. Carriles R, Schafer DN, Sheetz KE, Field JJ, Cisek R, Barzda V, Sylvester AW, Squier JA (2009) Invited review article: imaging techniques for harmonic and multiphoton absorption fluorescence microscopy. Rev Sci Instrum 80(8):081101
17. Zipfel WR, Williams RM, Webb WW (2003) Nonlinear magic: multiphoton microscopy in the biosciences. Nat Biotechnol 21 (11):1369–1377
18. Ehlers A, Riemann I, Stark M, König K (2007) Multiphoton fluorescence lifetime imaging of human hair. Microsc Res Tech 70 (2):154–161
19. Habenicht A, Hjelm J, Mukhtar E, Bergström F, Johansson LBÅ (2002) Two-photon excitation and time-resolved fluorescence: I. The proper response function for analysing single-photon counting experiments. Chem Phys Lett 354(5–6):367–375
20. Zheltikov AM (2006) Let there be white light: supercontinuum generation by ultrashort laser pulses. Phys Usp 49(6):605
21. Available from: http://www.picoquant.com/datasheets/photon_counting/PDM_Series.pdf.
22. Forest SE, Lam WC, Millar DP, Nofsinger JB, Simon JD (2000) A model for the activated energy transfer within eumelanin aggregates. J Phys Chem B 104(4):811–814
23. Zhang Q, Piston DW, Goodman RH (2002) Regulation of corepressor function by nuclear NADH. Science 295(5561):1895–1897
24. Arcangeli C, Yu W, Cannistraro S, Gratton E (2000) Two-photon autofluorescence microscopy and spectroscopy of Antarctic fungus: new approach for studying effects of UV-B irradiation. Biopolymers 57(4):218–225